Journal of Materials and Environmental Sciences
ISSN : 2028-2508

JMES, 2017 Volume 8, Issue 4, Page 1498-1507

http://www.jmaterenvironsci.com /

Elephant grass biomass extract as corrosion inhibitor for mild steel in acidic medium

E. B. Ituen[a,b*], A. O. James[c], O. Akaranta[b,c]

[a]*Materials Physics and Chemistry Research Laboratory, College of Science, China University of Petroleum, Qingdao, China.*
[b]*African Centre of Excellence in Oilfield Chemicals Research, Institute of Petroleum Studies, University of Port Harcourt, Nigeria.*
[c]*Department of Pure and Industrial Chemistry, University of Port Harcourt, Nigeria.*

Received 11 Mar 2016,
Revised 16 Sep 2016,
Accepted 25 Sep 2016

Keywords
- ✓ Adsorption,
- ✓ Green corrosion inhibitor,
- ✓ Elephant grass,
- ✓ Mild steel,
- ✓ Oilfield chemicals,
- ✓ Electrochemical techniques.

ebituen@gmail.com
Tel: +2348069762033

Abstract

Wild elephant grass species (*Pennisetum purpureum*) was extracted in acetone and investigated as alternative oilfield chemical for inhibiting the corrosion of mild steel surface in 3.5% HCl. Corrosion was monitored by Weight Loss (WL), Electrochemical Impedance Spectroscopy (EIS), Potentiodynamic Polarization (PDP) and Linear Polarization Resistance (LPR) techniques. Inhibition efficiency of elephant grass extract (EGE) up to 81.7% was obtained at 30^{o}C but this efficiency decreased as temperature increased. Increase in EGE concentration increased charge transfer resistance and decreased double layer capacitance. Adsorption isotherms and kinetic models were also used to describe the adsorption and activation processes. Results reveal that the presence of EGE increases the activation energy and reduces the rate corrosive attack of the acid on the steel specimens. EGE acts as mixed type inhibitor and was physically adsorbed on mild steel surface.

1. Introduction

Several chemicals which are utilized in the petroleum industry for various operations may be collectively referred to as oilfield chemicals. When existing fields deplete, the use of chemistry to maintain production becomes crucial and more economically viable than abandoning the well to drill new ones. During some operations like well stimulation, scale dissolution and enhanced oil recovery, some corrosive agents like water, carbon (iv) oxide and acid are introduced into the bore hole. The consequence of this is usually corrosion of metal structural facilities like casings and pipelines, many of which are made of steel [1]. Corrosion in oilfield has been implicated in a number of cost-increasing outcomes such as rupturing of pipelines and storage facilities, cost of managing/cleaning spills, shut down of plant for maintenance, loss of integrity of structures and flow problems [2-4]. Since no industry wants to risk any of these, proactive measures are usually employed to mitigate corrosion. Most industries prefer to use corrosion inhibitors to combat oilfield corrosion perhaps because the approach is easy and cost effective.

A corrosion inhibitor is a chemical substance which reduces the rate of metal dissolution in the medium it is employed. Efficient corrosion inhibitors can be obtained from chemical compounds which contain electron rich functionalities such as nitrogen, oxygen and/or sulphur atoms, multiple bonds, aromatic and/or heterocyclic rings [5]. However, most chemical inhibitors are toxic and very expensive. Many countries have placed restrictions on toxic corrosion inhibitors, therefore encouraging the use of green (ecologically friendly) ones. Being usually deployed in large quantities, cheap green corrosion inhibitors would also be economically desirable. Requirements such as non-toxicity, low cost and renewability are satisfactorily obtained from corrosion inhibitors sourced from local materials like agricultural wastes and plants extracts. In addition, commercialization of corrosion inhibitors sourced from local materials would create internal wealth, reduce importation rate and contribute to local content development.

However, extracts from plant biomass contain complex phyto-compounds that can be effective in corrosion inhibition [6-12] but are less efficient at high temperatures because increase in heat degrades these phyto-compounds [13]. This problem continues to limit the acceptability of corrosion inhibitors designed from plant

biomass. Survey of literature reveals that reduction in corrosion inhibitor effectiveness with increasing temperature is not only typical of plant extracts, but also occurs with some pure compounds and organic molecules [14-20].With the global scarcity of food which nations are trying to guard against, it is important that plants used for manufacture of corrosion inhibitors should not compete with food [13]. Therefore, in search for alternative corrosion inhibitors sourced locally, we investigated extracts from elephant grass biomass. Elephant grass is non-edible, easy to cultivate and asexually propagates very fast which make it a renewable source. It is not a cash crop and is usually regarded as weed and discarded or burnt off in farmlands and homesteads. Apart from for forage, the plant has been used as high energy plant for bioethanol, biofuel and biogas production [21-26], for sugar production [27-29], production of charcoal [30] and defluoridation of aqueous solutions [31]. The ashes have been used as supplementary cementing material [32] to improve the mechanical properties of cement [33] and to reinforce thermo-physical properties of some polymer composites [34-35]. Elephant grass fleshy stem is known to be rich in some water soluble vitamins [36]. Analysis of chemical composition of the plant extracts reveals that it contains some phyto-compounds (like anthocyanins and flavonoids) that are rich in electron donating sites [27, 36, 37-39] which also motivated its choice in the present study.

2. Experimental

2.1 Preparation of metal specimens

Mild steel sheets purchased from construction materials market in Uyo, Akwa Ibom state, Nigeria were used to simulate the pipework. The chemical composition of mild steel was C (0.13), Si (0.18), Mn (0.39), P (0.40), S (0.04), Cu (0.025), Fe (balance). They were mechanically press-cut into coupons of dimensions 4 cm x 4 cm and degreased in ethanol. Surface polishing was achieved using different grades of silicon carbide electro-coated water-proof abrasive papers and finished with CC-22F P1000 grade, cleaned with acetone, air-dried, weighed and immediately immersed in appropriate test solution. Another dimension (1 cm x 1 cm) was polished using machine and one surface exposed for electrochemical studies.

2.2 Preparation of test solutions

The corroding medium was simulated using 3.5% HCl prepared by diluting 37% analytical grade stock solution in distilled water. Mature elephant grass shoots harvested within University of Uyo community, Nigeria, were washed in distilled water, air-dried in the laboratory, grounded to powder and extracted in acetone by maceration, percolation and infusion [40]. Appropriate weights of the extract were prepared respectively in the acid to concentrations 0.1, 0.5, 1.0, and 5.0 g/L. All preparations were made using distilled water.

2.3 Gravimetric technique

Pre-weighed steel coupons were immersed completely in the 3.5 % HCl with and without the different concentrations EGE inside beakers containing about 100 mL of the solutions. They were retrieved after six (6) hours, washed in detergent solution, rinsed in distilled water, dried in air after rinsing in acetone and then reweighed. The differences in weights were recorded as weight loss. This procedure was followed for different temperatures (30, 40, 50 and 60 ^{o}C) maintained in water bath. All weights were obtained using Sartorius CPA225D analytical balance of sensitivity ± 0.01 mg. By denoting the initial and final weights of the coupons as W_1 and W_2 respectively, corrosion rates (R), percentage inhibitor effectiveness (inhibition efficiency), $\mathcal{E}_{WL}$ (%), and degree of surface coverage (θ) were calculated as follows:

$$R = (W_1 - W_2)/At \quad (1)$$

$$\varepsilon_{WL} = 100\left(\frac{R_b - R_i}{R_b}\right) \quad (2)$$

$$\theta = 0.01\varepsilon_{WL} \quad (3)$$

where R_b and R_i are the corrosion rates ($gcm^{-2}h^{-1}$) in the absence and presence of the inhibitor and $A$is the surface area (cm^2) of the metal specimens.

2.4 Electrochemical Impedance Spectroscopy

Gamry Potentiostat/Galvanostat/ZRA REF600-18042 electrochemical workstation with conventional three electrodes arrangement: saturated calomel electrode (SCE) as reference, platinum electrode as counter and mild

steel as working electrode with about 1.44 cm^2 exposed surface area. The system was allowed to attain the steady open circuit potential (OCP) between 0 and 1800 s before measurement was made. The EIS was conducted at frequency of 100 kHz to 10 mHz and amplitude voltage of 5 mV at room temperature (28 ± 1 ^oC). Experiments were conducted by complete immersion without stirring. The inhibition efficiency was calculated from charge transfer resistance values (Eq. 4) obtained using Echem Analyst version Gamry Application software package and data fitting of Nyquist and Bode plots.

$$\mathcal{E}_{EIS} = 100\left(\frac{R_{CTI} - R_{CTB}}{R_{CTI}}\right) \quad (4)$$

where R_{CTB} and R_{CTI} are charge transfer resistances in the absence and presence of inhibitor respectively

2.5 Potentiodynamic polarization measurement

The electrochemical same set up was used to obtain Tafel polarization curves at that temperature by changing electrode potential automatically from -250 mV to +250 mV vs. SCE at open circuit potential (OCP) with a scan rate of 1.0 mVs^{-1}. The corrosion current densities (I_{CORR}) were obtained from analyses of the Tafel plot at the point of intersection of anodic and cathodic curves using E-Chem software. The inhibition efficiency ($\mathcal{E}_{PD}$) was calculated from corrosion current density values (Eq. 5) obtained from data fitting with the software.

$$\mathcal{E}_{PD} = 100(1 - {}^{I_{CORRi}}/_{I_{CORRb}}) \quad (5)$$

where I_{CORRb} and I_{CORRi} are the corrosion current densities in the absence and presence of the inhibitor respectively.

2.6 Linear polarization resistance

This measurement was also used to study the corrosion behaviour of the inhibitor at that temperature. An electrode potential of ±20 mV vs OCP was maintained at a scan rate of 1.0 mVs^{-1}, Inhibition efficiency ($\mathcal{E}_{RP}$) was calculated from the polarization resistance obtained using Eq. 6.

$$\mathcal{E}_{RP} = 100\left(\frac{R_{Pi} - R_{Pb}}{R_{Pi}}\right) \quad (6)$$

Where R_{Pb} and R_{Pi} are the polarization resistances in the absence and presence of the inhibitor respectively.

3. Results and discussion

3.1 Gravimetric corrosion rate

Corrosion is an electrochemical process, hence gravimetric measurement presents a reliable approach to estimation of corrosion rates of an exposed surface area of a metal specimen in acid media as it directly relates loss in weight with time (corrosion rate) calculable electrochemical parameter like current density (j) (Eq. 7):

$$\frac{1}{A}\left(\frac{\partial W}{\partial t}\right) = j.\frac{M}{nF} \quad (7)$$

Where *M* is the molar weight of the metal (Fe) specimen.

The magnitudes of corrosion rates $\left(\frac{\partial W}{\partial t}\right)$ of the coupons calculated from weight loss values for all the test solutions are shown in Table 1. Corrosion rate increased with increase in temperature. The highest corrosion rate was obtained in the free acid solution. Therefore, the presence of EGE reduced the corrosion rates, implying that EGE actually retarded the mild steel corrosion. The effectiveness of the EGE increased with increase in concentration, showing that better inhibition efficiency could be obtained if EGE concentration is further increased. Similar trend has also been reported in literature [41-47].

3.2 Inhibitor effectiveness

The inhibitor effectiveness is measured in terms of percentage inhibition efficiency. The obtained values (Table 1) increased with increase in concentration of EGE and decreased with increase in temperature, which is consistent with other reports available in literature [48-51]. The decline in effectiveness of EGE with temperature is typical of most inhibitors from plant biomass. Further study is ongoing to formulate EGE with synergistic intensifiers aimed at improving on the obtained efficiency.

Table 1: Corrosion rate, inhibition efficiency and degree of surface coverage for mild steel corrosion in 3.5% HCl at different temperatures calculated from gravimetric measurement

C (g/L)	30°C			40°C			50°C			60°C		
	R (mgcm^{-2}h^{-1})	ε_{WL} (%)	θ	R (mgcm^{-2}h^{-1})	ε_{WL} (%)	θ	R (mgcm^{-2}h^{-1})	ε_{WL} (%)	θ	R (mgcm^{-2}h^{-1})	ε_{WL} (%)	θ
0.0EGE	2.313	-	-	5.174	-	-	13.134	-	-	27.538	-	-
0.1EGE	0.936	59.5	0.595	2.169	58.1	0.581	6.433	51.0	0.510	16.341	40.7	0.407
0.5EGE	0.830	64.1	0.641	1.917	62.9	0.629	5.478	58.3	0.583	13.072	52.5	0.525
1.0EGE	0.525	77.3	0.773	1.355	73.8	0.738	3.930	70.1	0.701	10.624	61.4	0.614
5.0EGE	0.381	83.5	0.835	0.945	81.7	0.817	3.007	76.6	0.766	9.035	67.2	0.672

3.3 Electrochemical Impedance measurement

Impedance measurement is a good technique in monitoring corrosion process. It is a non-destructive test because the magnitude of potential applied is small. Also, surface modification and errors associated with large deviations from electrochemical equilibrium are also reduced [52]. Information derived can be related to the kinetics of the electrode process, mechanism and surface properties at the metal/solution interface. Therefore, EIS tests were conducted. A plot of the imaginary against real impedance components afforded the Nyquist plot shown in Fig. 1. Also, Bode modulus (/Z/ vs. log f) and phase angle (phase angle vs. log f) plots was obtained in one frame of plot as shown Fig. 2 respectively and used to explain the corrosion process and its inhibition. Some of the EIS parameters obtained are shown in Table 2.

The diameters of the Nyquist plot curves produced imperfect semicircles. They were also different in sizes in the presence of the inhibitors from that of the free acid which portrays the influence of EGE on the corrosion of mild steel due to inhibition. The diameter increases as inhibitor concentration increases, corresponding to increase in inhibitive effect according to the trend 5.0 EGE > 1.0 EGE. The imperfections in shapes of the semicircles may be attributed to surface roughness or inhomogeneity of the mild steel [53]. A single capacitive loop obtained indicates that the corrosion process is mainly controlled by charge transfer process [54] and also that presence of EGE does not change the mechanism of the steel dissolution. Data obtained were also fitted into equivalent circuits; an excellent fit was obtained with the circuit represented in Fig. 3. The roughness or surface heterogeneity was compensated by a non-integer element dependent on frequency [55] called constant phase element (CPE) in the equivalent circuit with magnitude given by Y_0 and n, related to impedance by [14]

$$Z_{CPE} = = (Y_0)^{-1}(jw)^{-n} \quad (8)$$

where Y_0 is the CPE constant, w is the angular frequency, j is an imaginary complex number, $(j^2 = -1)\alpha$ is the phase angle of CPE and $n = 2\alpha/(\pi)$ is the CPE exponent.

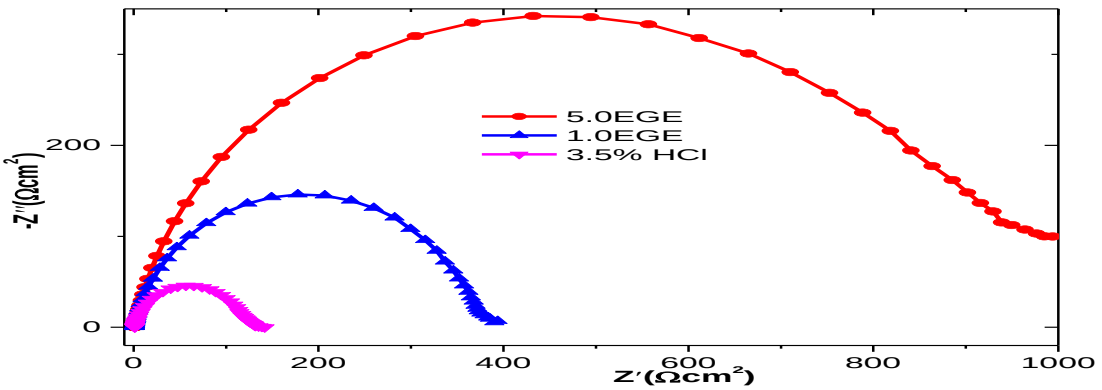

Figure 1: Nyquist plot for the corrosion of mild steel in 3.5% HCl in the absence and presence of different concentrations of EGE.

The values of n signifies deviation of the CPE and may be used to predict the degree of heterogeneity or roughness of the steel surface. It increases on addition of inhibitor than free acid solution indicating that the surface roughness of the mild steel is reduced by adsorption of EGE on its active sites [56]. Geethanjali and Subhashini have stated that when $n = 1$, Y_0 is capacitive; when $n = -1$, Y_0 is inductive; when $n = 0.5$, Y_0 is Warburg impedance [15]. Being in between these values, the obtained n values indicate relative and/or integrated influence of above factors such that it is not just a single resistance, capacitance or inductive element.

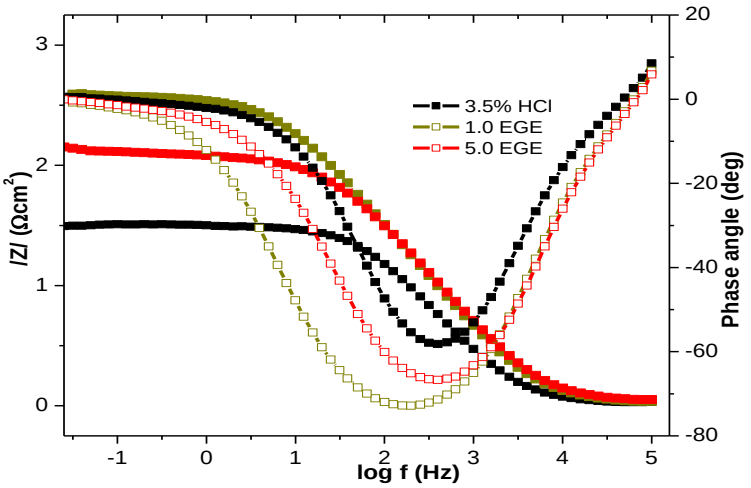

Figure 2: Bode and phase angle plots for the corrosion of mild steel in 3.5% HCl in the absence and presence of different concentrations of EGE.

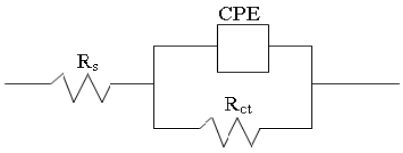

Figure 3: Electrochemical equivalent circuit used to fit Nyquist and Bode plots for corrosion of mild steel in 3.5% HCl in the absence and presence of different concentrations of EGE.

The value of n can also be corroborated to phase shift or deviation from ideal behaviour; increase on addition of inhibitor indicates insulation of the metal/solution interface which could have been caused by formation of a thin surface protective film responsible for the corrosion inhibition. This was evident in the charge transfer resistances obtained which increased in the presence of EGE than the free acid indicating concentration dependent retardation of steel dissolution rate by EGE. Increase in peak heights of the Bode plots also indicates more capacitive response of the interface due to the presence of adsorbed inhibitor layer and the magnitude of the capacitance was calculated from the peak angular frequency (w_{max}) using Eq. 9 below:

$$C_{dl} = Y_0 (w_{max})^{n-1} \quad (9)$$

The obtained C_{dl} values decrease on addition of inhibitor. This decrease could have been caused by either a decrease in the local dielectric (due to capacitive reactance) or an increase in the thickness of electrical double layer (adsorbed protective film) or both. The thickness (Δl) of which may be estimated using the Helmholtz model below [57].

$$\Delta l = (\varepsilon_0 \varepsilon A)/C_{dl} \quad (10)$$

where ε_0 and ε are the dielectrics of vacuum and the medium respectively and A is the electrode surface area. Inhibition efficiency obtained also increased with increase in concentration of EGE and virtually similar to those obtained with weight loss measurement.

Table 2: Parameters obtained from EIS measurement for mild steel in 3.5% HCl in absence and presence of different EGE concentrations.

EGE conc.	R_{CT} (Ωcm^2)	R_S ($m\Omega cm^2$)	Y_0 ($\mu\Omega^{-1}s^n$)	n	C_{dl} (μFcm^{-2})	ε_{EIS} (%)
0.0EGE	19.15	557.80	411.20	0.8820	4.02	-
1.0EGE	58.44	573.21	202.30	0.8715	2.18	67.23
5.0EGE	121.05	609.15	213.80	0.8503	0.93	84.12

3.4 Potentiodynamic polarization measurement

This measurement was carried out so as to study the effect of EGE on the anodic and cathodic reactions occurring in the system. For electrochemical dissolution of iron in hydrochloric acid, the following reactions are expected at the electrodes:

Anode: $Fe_{(s)} \rightarrow Fe^{2+}_{(aq)} + 2e$ (11)

Cathode: $2H^{+}_{(aq)} + 2e \rightarrow H_{2(g)}$ (12)

While anodic oxidation of the iron results in its dissolution (corrosion), hydrogen gas is liberated at cathode. The corrosion current density (I_{CORR}), corrosion potential (E_{CORR}), Tafel cathodic and anodic constants (β_c and β_a) and the percentage inhibition efficiency were obtained (Table 3). On addition of EGE, the I_{CORR} values strikingly shifted to lower current regions, the magnitude of which decreases with increase in inhibitor concentration while E_{CORR} shifted to higher values. Such behaviour demonstrates reduction of the mild steel corrosion by EGE. The E_{CORR} shifted towards the direction of more positive values, indicating that EGE has stronger effects on the anodic reaction than cathodic reaction. This may also be observed by ordinary inspection of the shapes of the curves in Fig. 4. Thus, EGE affects the rate of dissolution of iron into aqueous solution as well as rate of hydrogen liberation, with the former taking predominance. This may have happened by adsorption of EGE phyto-compounds on the steel surface resulting in inhibition of its corrosion. The obtained shift is less than 85mV hence not sufficient to ascertain whether the inhibitor is the cathodic or anodic type [58]. From these results, the adsorption of the inhibitor may have blocked both cathodic and anodic sites making it function as a mixed type with anodic dominance [14, 58]. The values of β_c and β_a obtained showed slight variations but with no particular trend. This implies that the inhibitor exhibited minor influence on the electrode reactions, maybe by geometric blocking of some active sites and not by change in mechanism [59]. Such influence may have also been due to slight modification caused by adsorption of the inhibitor and perhaps formation of an insulating protective film. The calculated inhibition efficiency increased with increase in concentration of the inhibitor. Similar trend have also been reported in literature [15, 58].

3.5 Linear polarization resistance

Polarization resistance was also measured for each of the test solutions. The obtained values (in Ω) were 22.18 for HCl, 154.44 for 1.0 g/L EGE and 191.15 for 5.0 g/L EGE corresponding to inhibition efficiencies of 85.2% and 88.4% for 1.0 g/L EGE and 5.0 g/L EGE respectively. This observation was attributed to the formation of a thin insulating protective inhibitor film at the mild steel-solution interface which offers considerable opposition leading to increase in R_p. This film could have been formed through adsorption of the inhibitor.

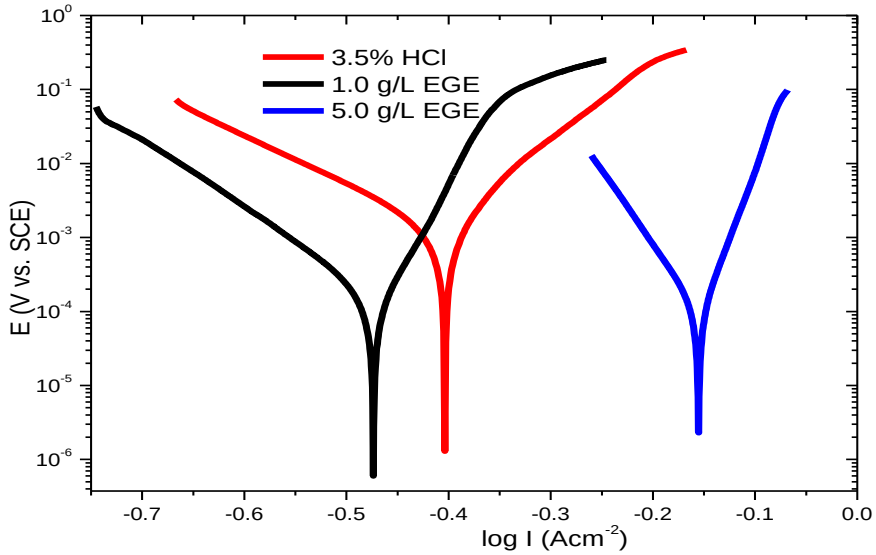

Figure 4: Tafel plots for mild steel in 3.5% HCl in absence and presence of different EGE concentrations.

Table 3 - Parameters obtained from PDP measurement for 3.5% HCl at different EGE concentrations.

EGE Conc. (g/L)	I_{CORR} (µAcm^{-2})	E_{CORR} (mV/SCE)	β_a (mVdec^{-1})	β_c (mVdec^{-1})	ε_{PD} (%)
0.00EGE	1390.0	-404	89.1	159.5	-
1.0EGE	252.0	-406	45.7	149.0	81.9
5.0EGE	129.0	-474	75.5	126.6	90.7

The differences in values of inhibition efficiencies obtained from polarization, impedance and weight loss measurements may have arisen because weight loss gives an average corrosion rate over a considerably longer

immersion time while electrochemical measurements give instantaneous corrosion rate, and time differences for the inhibitor to form the adsorbed layer on the metal surface [60].

3.6. Adsorption studies

The inhibition of mild steel corrosion by EGE extract is believed to proceed by initial adsorption on the steel surface and formation of a thin protective film that 'blankets' it from acid attack. The adsorbed film may comprise of a layer or more of the EGE molecules. To determine the nature of this layer and interactions within it, fractional surface values computed from weight loss data (Table 1) were fitted into various adsorption isotherm models (Fig 5). These models describe equilibrium relationships between amount adsorbed (θ) and equilibrium concentration (*C*) of inhibitor at a given temperature according to the general form given in equation (13) below:

$$f(\theta,x)e^{(-2a\theta)} = K_{ads}\,C \qquad (13)$$

where $f(\theta,x)$ represents the configuration factor which depends on the physical model and assumptions underlying the derivation of the particular model, K_{ads} is the adsorption equilibrium constant which describes how strongly the inhibitor molecules are held or bound on the steel surface and a is the molecular interaction parameter used to predict the nature of interactions in the adsorbed layer. Adsorption parameters computed (Table 4) were used to describe the nature and mechanism of adsorption from established principles.

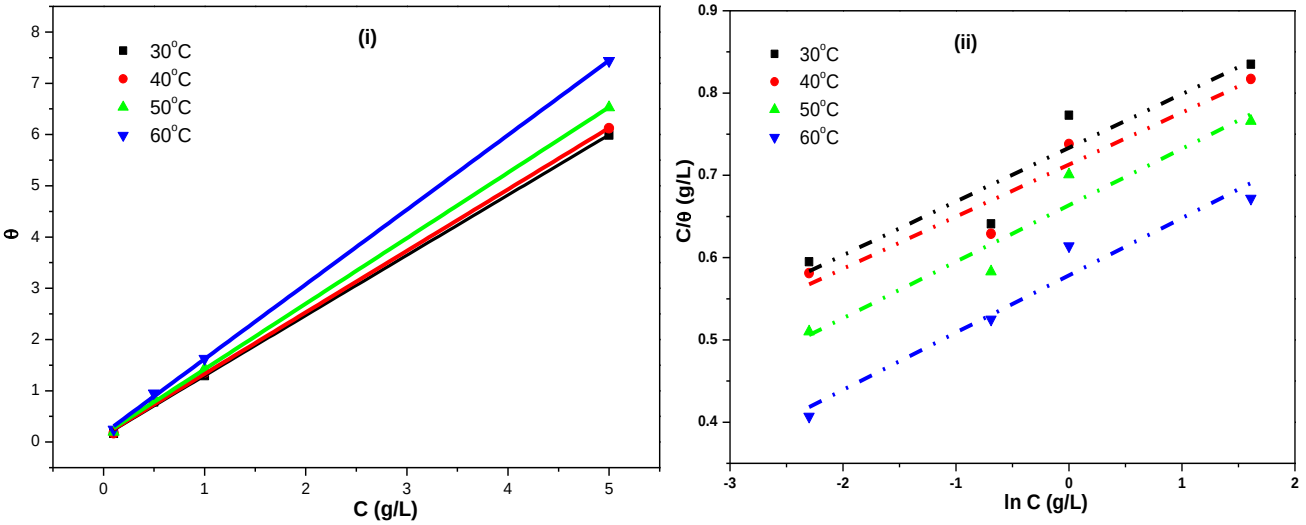

Figure 5: Langmuir and Temkin adsorption isotherms for adsorption of different concentrations of EGE on mild steel at different temperatures.

The data was first fitted into the Langmuir adsorption isotherm model which relates the fractional surface coverage to the concentration of the inhibitor according to equation (14) below.

$$\frac{C}{\theta} = 1/K_{ads} + C \qquad (14)$$

The Langmuir isotherm model assumes a monolayer adsorption of identical and equivalent inhibitor molecules at fixed number of definite localized adsorption sites with no lateral interaction or steric hindrance between them. All the sites on the adsorbent are also assumed to possess equal affinity for the adsorbate and constant sorption activation energy and enthalpy [61]. The inhibitor-steel binding equilibrium constant, K_{ads} values obtained indicate that binding strength between inhibitor and steel was moderate and decreased as temperature increased. Results also reveal non-unity slopes (1.17445 - 1.44712) which shows that there is interaction of the adsorbed species, one of the factors that were ignored while deriving the model. Therefore, the data was fitted into Temkin adsorption isotherm (Eq. 15) to describe the nature of the interactions. This afforded the lateral molecular interaction parameter (a) which indicates that repulsion may have taken place in the adsorbed layer with magnitude gradually declining with increasing temperature.

$$\theta = -\frac{1}{2a}\ln C - \frac{1}{2a}\ln K \qquad (15)$$

The values of K_{ads} obtained are shown in Table 4.

Table4: Adsorption parameters obtained from data fitting into adsorption isotherms

Model	Temp (^oC)	R^2	K_{ads} (M^{-1})	Slope	a
Langmir	30oC	0.99928	8.410	1.17445	-
	40oC	0.99926	7.643	1.19919	-
	50oC	0.99932	7.019	1.27895	-
	60oC	0.99833	4.701	1.44712	-
Temkin	30oC	0.84246	2.0826	0.06528	-7.6593
	40oC	0.89603	2.0410	0.06323	-7.0976
	50oC	0.90284	1.9422	0.06863	-7.2854
	60oC	0.93413	1.7836	0.06959	-7.1849

3.7 Effect of temperature and kinetic studies

Data fitting into Arrhenius activation model (Fig 6, Eq. 16) afforded parameters (Table 5) that provide possible explanations to the effect of temperature on the activation-controlled corrosion process and its inhibition from the collision theory point of view.

$$\log R_c = \log A - {}^{E_a}/_{2.303RT} \qquad (16)$$

Where A is the pre-exponential or frequency factor, R is the universal gas constant and T is the temperature.

For the acid to attack and corrode the mild steel surface there must be collision between both species. Successful acid molecules must possess a minimum energy equal to the activation energy (E_a^{HCl}) on collision with the metal surface. Higher activation energies were obtained with inhibited solution than E_a^{HCl}, implying that addition of inhibitor has increased the energy barrier that molecules of 1.0 M HCl must overcome in other to attack and corrode the mild steel surface or dissolve it. Thus, EGE introduction may have deepened the location of the Fe ions in the metal lattice energy well, increase the energy required to cross over and become metal cations, leading to the anti-corrosive effect. Typically, the pre-exponential factor expresses the fraction of the acid molecules that possess enough energy to attack the mild steel surface and dissolve it, as governed by the Maxwell-Boltzmann law, and can run between zero and unity (i.e. $0 \leq A \leq 1$), depending on the magnitude of activation energy and temperature. Our results are in agreement with these theoretical limits, implying adherence of EGE adsorption to the model. The free acid solution has the highest fraction of molecules with enough energy to attack the mild steel surface; hence the highest value of A. Decrease in magnitude of A with increase in concentration implies that the corrosion inhibitor would be more effective if concentration is increased.

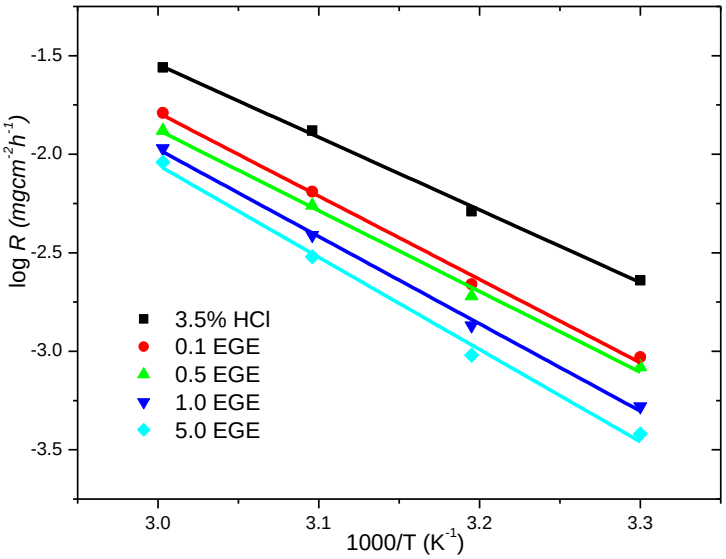

Figure 6: Arrhenius Plot for inhibition of mild steel corrosion in 3.5% HCl with and without different concentrations of EGE at 30°C to 60°C.

A decrease in inhibition efficiency with increase in temperature as well as higher activation energy of the uninhibited test solution than inhibited solution ($E_{a\,\text{uninhibited}} > E_{a\,\text{inhibited}}$) is associated with physical adsorption mechanism [62]. Thus, an increase in solution temperature decreases the number of adsorbed inhibitor

molecules, resulting in desorption and a decrease in inhibition efficiency. The EGE may have affected the inhibition efficiency either by decreasing metal surface available for acid attack (geometric blocking effect) or by modifying (increasing) the activation energy of the anodic or cathodic reactions occurring in the inhibitor-free surface [63]. Electrochemical results had earlier indicated that addition of the inhibitor effected slight modifications of the activation mechanism of the anodic reaction, hence coherency of our report. The higher activation energies imply increased energy barrier, slow reaction and sensitivity of reaction rate to temperature variations.

Table 5: Kinetic activation parameters derived from Arrhenius plot

Concentration	E_a (Jmol^{-1})	$A(x10^9)$
3.5% HCl	70.576	3.257
0.1 EGE	80.935	0.781
0.5 EGE	84.190	0.259
1.0 EGE	84.807	0.205
5.0 EGE	89.580	0.096

Conclusion

Extract of elephant grass biomass was investigated as alternative ecofriendly corrosion inhibitor. Elephant grass extract effectively inhibits the corrosion of mild steel in 3.5% HCl at 30 to 60 ^{o}C. Adsorption of EGE molecules is by spontaneous physical adsorption mechanism and is best approximated by the Langmuir adsorption isotherm. EGE behaves as a mixed-type corrosion inhibitor. EGE could be optimized to make an effective eco-friendly alternative oilfield corrosion inhibitor.

Acknowledgements-The financial support provided by World Bank Robert S. McNamara Fellowship Program 2015 to carry out this research abroad is gladly acknowledged. Dr. Shuangqing Sun of Materials Physics and Chemistry Research Laboratory, China University of Petroleum, Qingdao and members of his research group are also acknowledged for providing the facilities for this research. We also appreciate the assistance of Ubong Jerome Etim of State Key Laboratory of Heavy Oil Processing, UPC, Qingdao.

References

1. Ossai C. I., Boswell B., Davies I. J.,*Eng. Fail. Anal*.53 (2015) 36.
2. Fernandez I., Bairan J. M., Mari A. R.,*Construc. Build. Mater.*101 (2015) 772.
3. Akinyemi O. O.,Nwaokocha C. N.,Adesanya A. O.,*J. Eng. Sci.Technol*.7 (2012) 517.
4. NAICE Publication 2002 Supplementary Materials. FHWA-RD-01-156.
5. Finsgar M.,JacksonJ. *Corros. Sci.* 6 (2014) 17.
6. Soltani N.,Tavakkoli,N.,Kashani M. K., Mosavizadeh A., Oguzie E. E.,Jalali M. R., *J. Indus. Eng. Chem.* 20 (2014) 3217.
7. Hu Q.,Qiu Y., Zhang G., Guo X., *Chin. J. Chem. Eng.* 23 (20151408.
8. Anupama K. K.,Ramya K. K., Shainy K. M., Abraham J., *Mater. Chem. Phys*. 167 (2015) 28.
9. Bhawshar J., Jain P. K., Jain P., *Alexan. Eng. J.* 54 (2015) 769.
10. Grassino A.N., Halambek J., Djakovi S., Brncic S.R., Dent M., Grabaric Z., *Food Hydrocoloid.*, 52 (2016) 265
11. Shabani-Nooshabadi M., Ghandchi M. S., *J. Indus. Eng. Chem*. 31 (2015) 231.
12. El Hamdani N., Fdil R., Tourabi M., Jama C., Bentiss F., *Appl. Surf. Sci.* 357 (2015) 1294.
13. Sangeetha M., Rajendran S., Muthumegala T. S., Krishnaveni A., *Zast. Mater*.50 (2011) 3.
14. Fouda A. S., Shalabi K., Elewady G. Y., Merayyed H. F., *Int. J. Electrochem. Sci.* 9 (2014) 7038.
15. Geethajali R., Subhashini S., *Port. Electrochim. Act.* 33 (2015) 35.
16. Mistry B. M., Sahoo S. K., Kim D. H., Jauharia S., *Surf. Interface Anal*. 47 (2015) 706.
17. Popova A.,Christov M.,Vasilev A.,*Corros. Sci.* 94 (2015) 70.
18. Obi-Egbedi N.O.,Obot I. B.,Eseola A. O., *Arab. J. Chem*. 7 (2014) 197.
19. Gurten A. A.,Keles H.,Bayol E., Kandemirli F., *J. Indus. Eng. Chem.* 27 (2015) 68.
20. Khalifa O. R.,Abdallah S. M., *Portu. Electrochim. Act.*29 (2011) 47.
21. Dussadee N., Reansuwan K., Ramaraj R., *Biores. Technol*. 155 (2014) 438.

22. Scholl A. L., Menegol D., Pitarelo A. P., Fontana R. C., Filho A. Z., Ramos L. P., Dillon A. L. P., Camassola M., *Biores. Technol.* 192 (2015) 228.
23. Scholl A. L., Menegol D., Pitarelo A. P., Fontana R. C., Filho A. Z., Ramos L. P., Dillon A. L. P., Camassola M., *Indus. Crops Product.* 77 (2015) 97.
24. Strezov V., Evans T. J., Hayman C., *Biores. Technol.* 99 (2008) 8394.
25. Crespo E., Graus M., Gilman J. B., Lerner B. M., Fall R., Harren F. J. M., Warneke C., *Atmos. Environ.* 65 (2013) 61.
26. Eliana C., Jorge R., JuanP., Luis R., *Fuel.* 118 (2014) 4.
27. Li Y., Zhang Y., Zheng H., Du J., Zhang H., Wu J., Huang H., *Chin. J. Chem. Eng.* 23 (2015) 1188.
28. Menegol D., Scholl A. L., Fontana R. C., Dillon A. J. P., Camassola M., *Energy Conver. Manage.* 88 (2014) 1252.
29. Fontoura C. F., Brandão L. E., Gomes L. L.,*J. Clean Product.*96 (2015) 85.
30. Mesa-Pérez J. M. Cortez L. A. B., Marín-Mesa H. R. R. José D. P., Cascarosa M. R. E., *Appl. Therm. Eng.* 65 (2014) 322.
31. Manna S. D., Roy S., Adhikari P. B., *J. Taiwan Inst. Chem. Eng*. 50 (2015) 215.
32. Nakanishi E. Y., Frías M. M., Santos S., Rodrigues S. F., Rodríguez M. S., Savastano O., *Construc. Build. Mater.* 73 (2014) 391.
33. Cordeiro G., Chagas S., Caroline P., *Cement Con. Compos.*55 (2015) 331.
34. Ramanaiah K., Ratna P., Hema A. V., Reddy C. K., *Mater. Let.* 89 (2012) 156.
35. Ridzuan M. J. M., Abdul Majid M. S. M., Afendi A., Kanafiah S, N., Zahri A. G., *Mater. Design*. 89 (2016) 839.
36..Akah N. P, Onweluzo N. J. C. *Nig. Food J.* 32 (2014) 120.
37. Tessema Z. R.,Baars M. T., *Ani. Feed Sci. and Technol*. 117, 1-2 (2004) 29.
38. Kabi F., Bareeba F. B., Havrevoll Ø., Mpofu I. D. T., *Livest. Produc. Sci.* 95 (2005) 143.
39. Akah N. P., Ani J. C., Third Int. Confer. Biodiv. UN Mille. Dev. Goals, 29-31 October (2014) France.
40. Handa S. S.,Khanuja S. P. S., Longo G.,Rekesh D. D., ICS-UNIDO (2008) 67.
41. Yan M., C. Sun J. Xu W. K., *Indus. Engin. Chem. Resear.*53, (2014) 17615.
42. Prasiai D.,Tuberquia C. J., Harl R. R., Jennings G. K., Rogers B. R.,Bolotin K. I., *ACS Nanotechnol.*6 (2012) 1102.
43. Balan P., Raman R. K., Chan E. S., Harun M. K.,Swamy V., *Prog. Organic Coat.*90 (2016) 222.
44. Shukla S. K.,Ebenso E. E., *Int. J. Electrochem. Sci.* 6 (2011) 3277.
45. Fouda A. S., Elmorsi M. A., Elmekkawy A., *Afri. J. Pure Appl. Chem.* 7 (2013) 337.
46. Bhat J. I., Alva V. D. P., *J. Korean Chem. Soc.* 55(2011) 835.
47. Zhang H., Pang X., Zhou M., Liu C., Wei L.,Gao K.,*Appl. Surf. Sci.* 356 (2015) 63.
48. Samide A. P., Bibicu I., *Surf. Interface. Anal.*40 (2008) 944.
49. Umoren S. A., *J. Appl. Polym. Sci.* 119 (2011) 2072.
50. Migahead M. A., Sabagh A. M., Khamis E. A., Zaki E. G., *J. Mol. Liq.* 212 (2015) 360.
51. Sigircik G., Tuken T., Erbil M., *Corros. Sci.* doi:10.1016/j.corsci.2015.10.036.
52. Orazem M. E., Tribollet B., Hoboken: John Wiley and Sons, 2008.
53. Yurt A., Ulutas S., Dal H., *Appl. Surf. Sci.* 253 (2006) 919.
54. Behpour M., Ghoreishi S. M., Mohammed N., Soltani N., Salavati-Niasari M.,*Corros. Sci.* 52 (2010) 4046.
55. Trinstancho-Reyes J. L., Sanchez-Carrillo M., Sandoval-Jabalera R., Orozco-Carmona V. M., Almeraya-Calderon F., Chacon-Nava J. G., Gonzalez-Rodriguez J. G., Martinez-Villafane A., *Int. J. Electrochem. Sci.* 6 (2011) 419.
56. Zarrok H., Zarrouk A., Hammouti B., Salghi R., Jama C., Bentiss F., *Corros. Sci.* 64 (2012) 243.
57. ShabanS. M., Aiad I., El-Sukkary M. M., Soliman E. A., El-Awady M. Y., *J. Mol. Liq.* 203 (2015) 20.
58. Mourya P., Banerjee S., Singh M. M., *Corros. Sci.* 85 (2014) 352.
59. Bai L.,Feng L. J., Wang H. Y., Lu Y. B., Lei X. W., Bai F. L., *RSC Advan.*5 (2015) 4716.
60. Zhang J., Song Y., Su H., Zhang L., Chen G., Zhao J., *Chem. Central. J.* 7 (2013) 109.
61. Deyab M A., *J. Power Sources*. 292 (2015) 66.
62. Ituen E. B., Udo U. E., Odozi N. W., Dan E. U., *J. Appl. Chem.*3 (2013) 52.
63. Solomon M. M., Umoren S. A., Udousoro I. I., Udoh A. P., *Corros. Sci.* 52 (2010) 1317.